Current Biology, Vol. 13, 1669–1678, September 30, 2003, ©2003 Elsevier Science Ltd. All rights reserved. DOI 10.1016/j.cub.2003.09.027

Mathematical Modeling Suggests Cooperative Interactions between a Disordered Polyvalent Ligand and a Single Receptor Site

Peter Klein,[1,2,*] Tony Pawson,[3,4] and Mike Tyers[3,4]

[1]Fox Run Management, LLC
35 Fox Run Lane
Greenwich, Connecticut 06831
[2]Center for Biomedical Engineering
Massachusetts Institute of Technology
77 Massachusetts Avenue
Cambridge, Massachusetts 02139-4307
[3]Samuel Lunenfeld Research Institute
Mount Sinai Hospital
600 University Avenue
Toronto, Ontario M5G 1X5
[4]Department of Medical Genetics and Microbiology
University of Toronto
1 Kings College Circle
Toronto, Ontario M5S 1A8
Canada

Summary

Background: The CDK inhibitor Sic1 must be phosphorylated on at least six sites in order to allow its recognition by the SCF ubiquitin ligase subunit Cdc4. However, because Cdc4 appears to have only a single phosphoepitope binding site, the apparent cooperative dependence on the number of phosphorylation sites in Sic1 cannot be accounted for by traditional thermodynamic models of cooperativity.

Results: We develop a general kinetic model, which predicts an unexpected multiplicative increase in affinity as a function of ligand sites. This effect, termed allovalency, derives from a high local concentration of interaction sites moving independently of each other. Modeling of this interaction by a first exit time approach indicates that the probability of ligand rebinding increases exponentially with the number of sites. This type of interaction is relatively immune to loss of any one site and may be easily tuned to any given threshold by adjusting the properties of individual sites.

Conclusions: The allovalency model suggests that a previously undescribed mechanism may underlie certain cooperative interactions. The widespread occurrence of flexible polyvalent ligands in biological systems suggests that this principle may be broadly applicable.

Introduction

Cooperativity is an essential feature of many biochemical systems [1]. This property, more generally described as ultrasensitivity by Goldbeter and Koshland [2–4], filters out low levels of noise and yields a maximal response over a narrow range of stimulus. Elaborate assemblies of ultrasensitive elements in combination with feedback loops may underlie all-or-none biological responses, which often occur at the cellular level during development [5, 6]. Several biochemical mechanisms can produce ultrasensitivity, including zero-order kinetics, second- and higher- order dependence on enzyme concentration, stoichiometric inhibitors, positive feedback, and protein translocation [4, 7].

Cooperativity can also arise when several small, single-dentate molecules bind to a large, polydentate molecule such that an early binding event increases the affinity of later binding interactions [8, 9]. Such cooperativity may result from contributions to binding energies from secondary substrate interactions or from allosteric effects, as in the case of oxygen binding by hemoglobin. Thus, the binding of the first O_2 molecule to one subunit of a hemoglobin tetramer enhances the affinity of the remaining subunits for O_2 and so on. This form of cooperativity requires ligand-induced changes in protein conformation [10]. Two general and well-known models have been proposed for the case in which many distinct ligands bind to a multimeric macromolecule in a cooperative way. In the MWC model, the first ligand to bind induces a concerted change in the conformation of the macromolecule to a state that has increased affinity for additional ligands. In the KNF model, only the subunit that binds the ligand is conformationally altered, and this causes a change in the interactions between the subunits such that subsequent ligand binding can have either higher or lower affinity [8].

Cooperativity is often at play in protein-protein interactions. For example, once seeded at appropriate monomer concentrations, assemblies of tubulin or actin have a strong tendency to polymerize [11]. The interactions of polyvalent ligands with protein multimers may in principle show a cooperative dependence on the number of binding sites; this effect is termed avidity in the context of antibody-antigen or virus-host interactions [1]. Cooperative interactions also occur in signaling pathways. For example, the 14-3-3ζ protein interacts with two distinct phospho-Ser sites on some of its ligands [12], whereas the phosphatase SHP2 uses its dual SH2 domains to engage two phospho-Tyr motifs on its targets [13]. Cooperativity in each of these situations arises from the increase in free energy summed over two or more discrete binding interactions and a resultant multiplicative increase in overall binding affinity.

Intrinsically disordered domains often play important roles in biological responses, particularly in cell signaling and regulation. It has been estimated that as many as 30% of proteins in eukaryotes consist of at least in part disordered domains while as many as 6% of proteins in yeast are completely disordered [14]. Many disordered proteins adopt folded structures upon binding to targets [15]. Lack of structure in an unbound state may have functional advantages such as the ability to bind several targets (sometimes called one-to-many signaling), thermodynamic control of binding, rapid recycling of excess protein, and inducibility through mechanisms such as phosphorylation [16]. It is conventional to think of cooperativity in this context as a result of the

*Correspondence: pklein@foxrunlp.com

simultaneous binding of several sites on the ligand to several corresponding sites on the receptor. However, another possible mechanism, namely, the cooperative binding of a polyvalent ligand that is intrinsically disordered to a single receptor with a single binding site, has not been examined in detail, nor to our knowledge has a detailed theoretical framework for the properties of such interactions been described.

Recent analysis of the yeast cell cycle has revealed a protein-protein interaction that exhibits apparent cooperative effects, namely, the binding of multiply phosphorylated forms of the cyclin-dependent kinase (CDK) inhibitor Sic1 to the F box protein Cdc4 [17]. At the point of cell cycle commitment in late G1 phase (Start), G1 forms of CDK activity phosphorylate Sic1 and thereby target it for ubiquitination by the SCF^{Cdc4} complex and subsequent rapid degradation by the 26 S proteasome [18–20]. Elimination of Sic1 liberates S phase CDK activities necessary for the initiation of DNA replication [21]. Unlike characterized phosphorylation-dependent protein interactions, in which a single phosphorylated residue forms a high-affinity binding epitope for a dedicated recognition domain [22], the mechanism of phospho-Sic1 recognition by Cdc4 requires phosphorylation of Sic1 on at least six of its nine possible CDK phosphorylation sites, termed Cdc4 Phospho-Degron (CPD) sites [17]. Intriguingly, the phosphorylation dependence of the Sic1-Cdc4 interaction is highly nonlinear. That is, when Sic1 is phosphorylated on five or fewer sites, little or no binding occurs, whereas when six or more sites are phosphorylated, maximal binding occurs. The requirement for phosphorylation on six sites may render the forward reaction dependent on the sixth order of kinase concentration, which in turn may confer switch-like onset of DNA replication [4, 17]. Experimental evidence suggests that the apparent cooperativity in the Sic1-Cdc4 interaction is neither due to multiple binding sites on Cdc4 [23] nor to allosteric changes in Sic1, which completely lacks secondary structural elements ([17], W.-Y. Choy and J. Forman-Kay, personal communication). It is also unlikely that either the MWC or the KNF molecular model of cooperativity is applicable [8, 10], since the size of the SCF^{Cdc4} complex probably precludes simultaneous binding of more than one Cdc4 molecule to Sic1 and since the structure of Cdc4 is not altered upon ligand engagement [23]. Thus, the known mechanisms that might account for cooperativity appear not to operate in this case. In order to provide a possible explanation for the cooperative transition in Sic1 recognition by Cdc4, we have developed a general mathematical model to account for the properties of an interaction between a disordered polyvalent ligand and a single-site receptor.

Results

Assumptions

In order to mathematically model the Sic1-Cdc4 interaction, we make a number of simplifying assumptions, which also serve to make the analysis applicable to any flexible, polyvalent ligand that interacts with a single binding site. We represent Sic1 as a cluster of nine, or more generally n, phosphorylation-dependent interaction sites (generically termed ligand or L sites) arranged on a fully flexible linear molecule, like beads on a string. To model the simplest possible interaction scenario, we assume that only a single ligand site on any given Sic1 molecule can interact with the single binding site on Cdc4 (generically termed the receptor or R site) at any given time. Each ligand site is assumed to bind the single receptor site with the same on and off rates, termed k_1 and k_{-1}, respectively. We consider each ligand to always be in one of two states: either inside an imagined sphere of suitably chosen radius r centered on the one receptor binding site, or outside any such sphere. Here, the term state is used in the general sense of stochastic processes, not in the sense of thermodynamics; thus, we do not assume that there is a free energy differential between the exterior and the interior of the sphere. The precise value of r is not critical, as we show, but is chosen to correspond to the estimated mean square end-to-end distance of the ligand molecule. The state in which the ligand is inside the sphere centered on the receptor is further divided into two substates; in the first, denoted B = Bound, one of the multiple ligand sites is bound to the one receptor site, in the other, P = Proximate, none of the sites are bound. The second state described above is called F = Free (Figures 1A and 1B). In state P, the various ligand binding sites are considered to be moving independently of each other, each one free to bind to the site on the receptor, and are constrained only by the requirement that all sites remain in the sphere until the whole ligand transitions to the F state. We also assume that each entry into state P occurs at the center of the sphere, so that a ligand that rebinds to the receptor is "recentered" prior to reentering the P state. We ignore any potential reduction in entropy during binding to the receptor and assume that diffusion is of a simple Smolukowski type without contributions from electrostatic or desolvation effects. Thus, all unoccupied spheres are encountered by ligand molecules at the diffusion rate. The cluster of n sites on a ligand in the P state will be considered a solution of local molar concentration $n/N_A \div (4\pi r^3/3 \times 10^3)$ mol L^{-1}, where N_A is Avogadro's number and r is in meters. The mean-square end-to-end distance for a random-coil polymer is given as Nl^2, where N and *l* are the number and length of residues, respectively [24]. In the instance of Sic1, the sufficient N-terminal targeting region of 90 residues contains seven CDK sites [18], six of which must be phosphorylated for Cdc4 binding to be detected [17]. Setting N = 90 and *l* = 3.5 Å for a fully extended amino acid residue yields an estimated mean end-to-end distance of approximately 33 Å. Using r = 35 Å and n = 7, the local molar concentration of binding sites for each Sic1 molecule is 6.47×10^{-2} mol L^{-1}. We use the value 5×10^{-11} m^2 s^{-1} for the diffusion coefficient of both ligand and receptor. The hydrodynamic radius of a disordered 130 residue fragment of a fibronectin binding protein has been given as 26.2 Å [25]. This value can be used in the Stokes-Einstein formula to calculate a diffusion coefficient of 8.4×10^{-11} m^2 s^{-1} in water. It is conceivable that the addition of phosphate groups to Sic1 add measurably to the hydrodynamic radius and that "molecular crowding" might reduce the diffusion

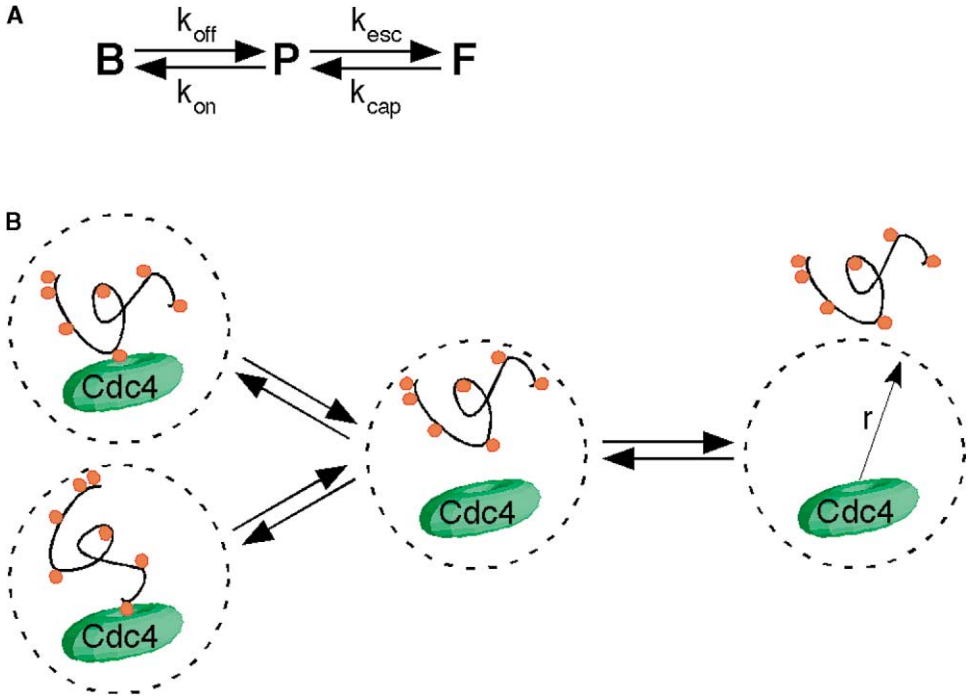

Figure 1. Principle of Allovalent Interactions

(A) A diagram of the three states (B = Bound, P = Proximate, and F = Free), transitions between each state, and their respective rate constants.

(B) A cartoon representation of the transition from a bound state to the proximate state defined by radius = r and either back to a second bound state or escape to the free state outside of radius = r.

coefficient three- to ten-fold compared to its value in water [26].

The Model

To model the dynamics of the ligand-receptor Sic1-Cdc4 interaction, we assume that the transitions in the reaction diagram (Figure 1A) follow simple rate laws (Equations 1a–1d). We use the standard steady-state assumption to derive an expression for the association constant $K_a(n)$ as a function of the number of ligand binding sites, n. The four individual state transitions in the model are described by:

$$\text{velocity}_{B\to P} = k_{off}\,[B] \quad (1a)$$

$$\text{velocity}_{P\to B} = k_{on}\,[P] \quad (1b)$$

$$\text{velocity}_{P\to F} = k_{esc}\,[P] \quad (1c)$$

$$\text{velocity}_{F\to P} = k_{cap}\,[L_f][R_f] \quad (1d)$$

Here, [R] and [L] are the total concentration of receptor (Cdc4) and ligand (Sic1), respectively, while $[R_f]$ and $[L_f]$ denote the concentration of free receptor and ligand, respectively, and satisfy:

$$[R_f] = [R] - [B] - [P] \quad (2a)$$

$$[L_f] = [L] - [B] - [P]. \quad (2b)$$

We compute the local concentration of Sic1 in the P state (r = 35 Å) as $1/(N_A \times 4\pi r^3/3 \times 10^3) \approx 9.246 \times 10^{-3}$ mol L^{-1}. Of the four rate constants in (Equations 1a–1d), two, k_{off} and k_{cap}, do not depend on the number of sites, while the two others, k_{on} and k_{esc}, do and are denoted $k_{on}(n)$ and $k_{esc}(n)$, where n is the number of binding sites (however, for simplicity, we allow n to vary continuously). For k_{on}, this is straightforward (Equation 3b); we will discuss in detail how $k_{esc}(n)$ varies with n. We emphasize that this dependence on n is a key distinguishing feature of the model. The rate constants k_{off} and k_{on} can be written:

$$k_{off} = k_{-1} \quad (3a)$$

$$k_{on}(n) = n \times k_{on}(1) = n \times k_1/(N_A \times 4\pi r^3/3 \times 10^3) = n \times k_1 \times 9.246 \times 10^{-3}, \quad (3b)$$

where k_{-1} and k_1 are the off and on rates, respectively, for a single binding site. A note about units: k_1 and k_{cap} are second-order reactions with units $mol^{-1}\ L\ s^{-1}$, while k_{-1}, k_{off}, $k_{on}(n)$, and $k_{esc}(n)$ are all first-order reactions with units s^{-1}.

The Source of Nonlinearity

In the above model, k_{on} varies linearly with n, the number of sites (Equation 3b), while k_{off} is independent of n (Equation 3a); so, to explain the nonlinearity of binding, we consider the rates at which the ligand enters and exits the sphere around the receptor, as described by k_{esc} and k_{cap}. Since the ligand comes into contact with the receptor through diffusion, we set k_{cap} equal to the

rate derived for a diffusion-controlled reaction [27]:

$$k_{cap} = 4\pi r(D + D_R)N_A, \quad (4)$$

where D and D_R are the diffusion coefficients for the ligand and the receptor, respectively, and N_A is Avogadro's number. We note that this rate depends primarily on hydrodynamic properties of the ligand and receptor, and therefore it is assumed to be independent of the parameter n. In contrast, we show that k_{esc} varies with n in an exponential fashion. It is important to understand that this does not mean that ligands diffuse slower out of P for increasing n, rather it is a consequence of the increased probability of rebinding to the receptor prior to leaving the sphere. We also note that it might seem contradictory that k_{esc} depends on n while k_{cap} does not, since balance of mass requires that in a steady state the right sides of Equations 1c and 1d are equal. However, since the concentrations [P], [L_f], and [R_f] all are free to vary with n, there is no paradox.

Velocities of first-order reactions depend only on the concentration of the initial reactant. This is typically thought to mean that any one molecule in the reactant state has the same probability as any other to transition to the product state. The reaction described in Equation 1c differs in the important respect that not all members of the state P are equally likely to transition to the F state. The longer a ligand has been in the P state, the more likely it is that the molecule will have had time to partially diffuse away from the immediate neighborhood of the binding site on the receptor and thus increase its chance of an escape from its former binding partner altogether. Thus, if rebinding to the receptor is rapid, there is less opportunity for the ligand to diffuse out of the P state. In terms of rate constants, k_{esc} (n) increases with the mean time to rebinding, or $1/k_{on}(n)$, i.e., $k_{esc}(n)$ varies inversely with n. We next show that $k_{esc}(n)$ declines as the exponential of negative n, i.e., $k_{esc}(n) \approx Ce^{-cn}$. This exponential property is sufficient to account for the cooperative nature of the binding curve.

Properties and Derivation of k_{esc}

The mean time for a particle diffusing with coefficient D to exit from a sphere of radius r centered at the particle's original position [28, 29] is given by:

$$\langle t \rangle = r^2/6D. \quad (5)$$

Substitution of reasonable experimental parameters in this equation suggests that in the case of a sphere around Cdc4, rebinding of Sic1 will occur much more quickly than diffusion away from the sphere (Figures 2 and 3). The critical variable to explain the ultrasensitive property of the rebinding transition is the distribution of time to first exit for a diffusion process, termed the "first exit time." We derive an expression for k_{esc} through the use of the Laplace transform and Bessel functions.

There is to our knowledge no explicit formula for the first exit time from a three-dimensional sphere, but it is clear that the general shape of this distribution should be similar to the one-dimensional first exit time for which there exists an exact formula (Figure 3). Exit from the sphere is a highly unlikely event for short time periods, but the frequency then rises to maximum, after which it quickly tapers off toward zero. This distribution is markedly different from the exponential distribution used to model the P → B transition, in which the probability per unit time of transition is at a maximum at time zero, after which it quickly tapers off (Figures 2A and 2B). It is the relationship between these two qualitatively different frequency distributions that causes k_{esc} to depend on $k_{on}(n)$.

Consider the Brownian motion originating at the center of a sphere of radius r at time 0 with diffusion coefficient D. We use this process to model the time for a ligand to exit the sphere. Denote by $f(\tau) = f(r, \tau)$ the frequency distribution of time until first exit from the sphere of such a motion. Because r is fixed, it can be suppressed. Let $\phi(\tau)$ be the "survivor" function associated with f, i.e.,

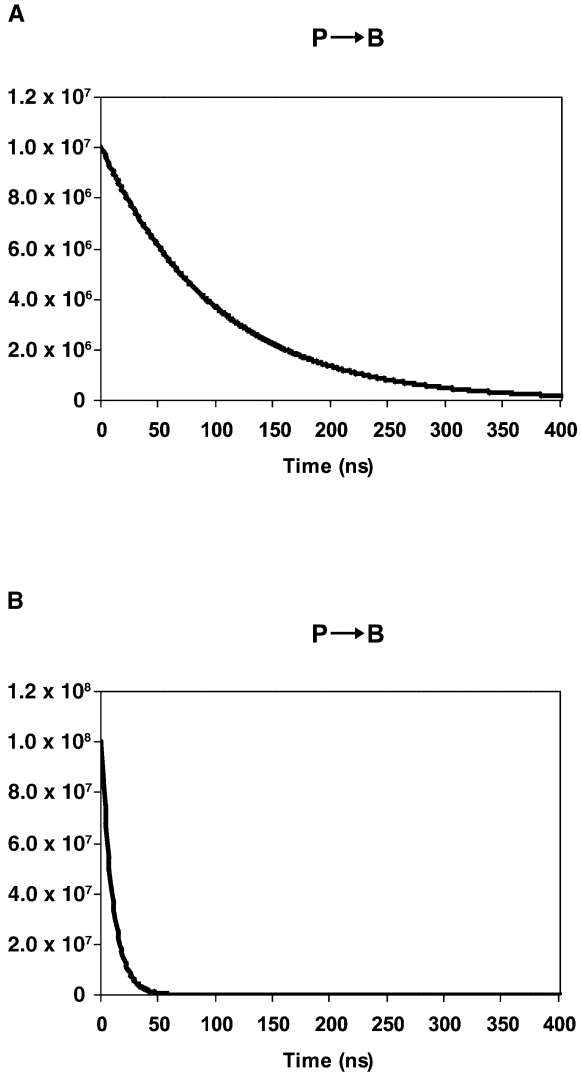

Figure 2. Probability Distributions of Transitions between the P and B States

(A) For the P to B transition with $p(t) = k_{on}\exp(-k_{on}t)$ and $k_{on} = 10^7$, mean = 100 ns.

(B) For the P to B transition with $p(t) = k_{on}\exp(-k_{on}t)$ and $k_{on} = 10^8$, mean = 10 ns. Note the different scale of the *y* axes in (A) and (B).

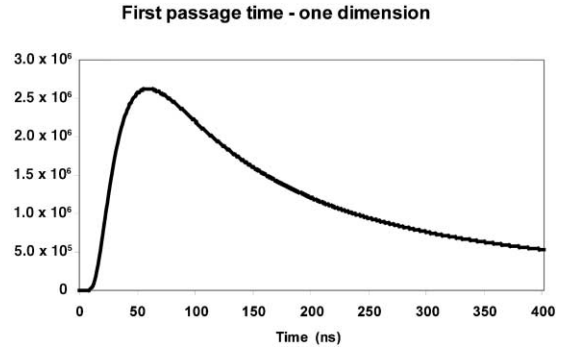

Figure 3. Time to First Exit

Time to first exit through a one-sided barrier for a diffusion process in one dimension:

$$p(t) = r/\sqrt{2\pi t^3}\,\exp(-r^2/2t).$$

$$\phi(\tau) \equiv 1 - \int_0^{\tau} f(y)dy = \int_{\tau}^{\infty} f(y)dy.$$

$\phi(\tau)$ thus represents the probability for a diffusing particle to remain within a sphere of radius r around its point of origination throughout time τ. For the ligand to have a reasonable probability to exit the sphere, it must occupy the P state for a certain time period. Whether or not a transition from P to F will take place during a small time interval, Δt depends not only on the length of the time interval Δt, but also on how long the state P has been occupied. In particular, the P → F transition is non-Markovian.

To describe the rate of escape from the state P, we introduce the probability density of "ages" for a ligand in state P, termed $a_t(\tau)$. The variable τ, ranging from 0 to ∞, will be used to denote the age of the ligand, while t will denote the current time in the system. Specifically, $a_t(\tau)$ is the fraction of all ligands in P at time t that entered P at time $t - \tau$ and remained in P until time t (i.e., is of age τ). We then assume that the system is in a steady state and set $a_t(\tau) = a(\tau)$ for all values of t. By definition, the concentration of ligands in P with ages in the interval $[\tau, \tau + \Delta\tau]$ is $a(\tau)\Delta\tau[P]$. In Appendix A (see the Supplemental Data available with this article online), we derive:

$$k_{esc} = \int_0^{\infty} \frac{a(\tau)f(\tau)}{\phi(\tau)}d\tau. \qquad (6)$$

The probability density $f(\tau)$ depends on the diffusion constant D, but not on the number of ligand sites, n. The sensitivity of k_{esc} to n thus comes solely from $a(\tau)$. We then derive a differential equation (A.6) (see Appendix A) satisfied by $a(\tau)$. In Appendix B (see the Supplemental Data), we use these results to derive an exact expression for k_{esc}:

$$k_{esc} = k_{on} \times \frac{1}{\dfrac{I_{1/2}(r\sqrt{\frac{k_{on}}{D}})2^{1/2}\Gamma(3/2)}{(r\sqrt{\frac{k_{on}}{D}})^{1/2}} - 1}, \qquad (B.19)$$

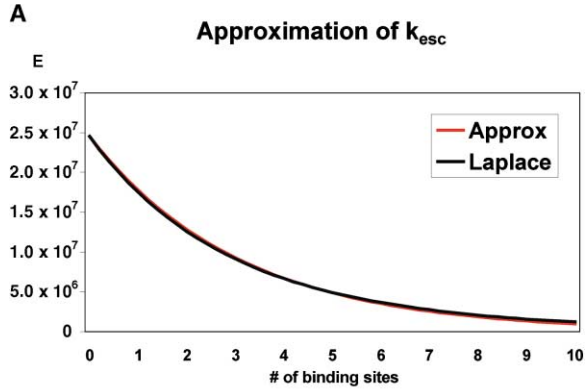

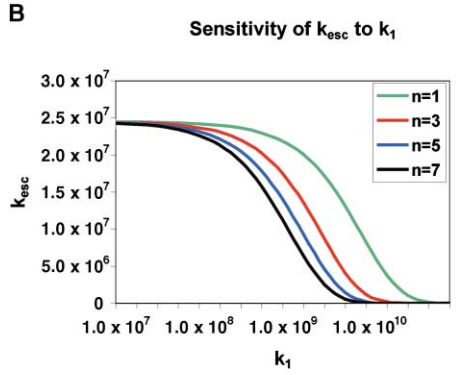

Figure 4. k_{esc} Varies Exponentially with n for a Range of Values for k_1

(A) Approximation of k_{esc}. The curve shown is for

$$k_{esc}(n) = k_{on} \times \frac{1}{\dfrac{I_{1/2}(r\sqrt{\frac{k_{on}}{D}})2^{1/2}\Gamma(3/2)}{(r\sqrt{\frac{k_{on}}{D}})^{1/2}} - 1} \qquad (B.19)$$

as compared to the approximation (7) $e(n) = \exp(-k_{on}(n)\omega/35)/\omega$ for r = 35 Å, D = 5×10^{-11} m^2/s, ω = 40.8 ns, and $k_1 = 3 \times 10^9$ s^{-1}; $k_{on}(1) = 2.77 \times 10^7$.

(B) Sensitivity of k_{esc} to k_1 for r = 35 Å, D = 5×10^{-11} m^2/s, and ω = 40.8 ns.

where $I_{1/2}$ is the modified Bessel function of the first kind of order 1/2 and Γ is the gamma function (see the Supplemental Data). To see that this is essentially an exponential function, we compare this expression for $k_{esc}(n)$ to the expression in (Figure 4A):

$$k_{esc}(n) \approx \frac{\exp(-k_{on}(n)\omega/35)}{\omega}, \qquad (7)$$

where $\omega = r^2/6D$ or the mean exit time. Equation B.19 shows that the escape rate depends on the on rate and the ratio of the on rate to the diffusion coefficient of the ligand.

K_a — The Apparent Association Constant

We now derive an expression for the apparent association constant as a function of n and demonstrate that

under reasonable experimental parameters, this expression can produce an ultrasensitive response. In a steady state, the concentrations of the B, P, and F states are constant, and we can write the two equations:

$$d[P]/dt = k_{off}[B] - k_{on}[P] - k_{esc}[P] + k_{cap}[L_f][R_f] = 0$$
$$d[B]/dt = k_{on}[P] - k_{off}[B] = 0. \quad (8)$$

From these, we deduce an expression for the association constant of complex formation:

$$K_a = ([B] + [P])/([L_f][R_f]) = (1 + k_{on}/k_{off})k_{cap}/k_{esc}\ (mol^{-1}L). \quad (9)$$

We note that this constant represents a kinetic equilibrium in that the concentrations of states are constant but not necessarily in thermodynamic equilibrium. From our previous discussion, we can conclude that $K_a \approx Cne^n$.

In order to find an expression for the fraction bound ligand, we combine the first part of Equation 9 with Equation 2b and derive the expression:

$$\%\ \text{Bound ligand} = ([B] + [P])/[L] = [R_f]/(1/K_a + [R_f]) = \frac{1}{1 + \frac{1}{K_a[R_f]}}. \quad (10)$$

We note that we have defined a ligand in state P as still being "bound" to the receptor. It is debatable whether detection of binding both in vitro and in vivo is sensitive enough to discriminate between P and B. In any case, replacing [B] + [P] with [B] in Equation 10 does not alter the model materially. Because K_a increases exponentially with n, the ligand binding response is rendered ultrasensitive with respect to the number of sites on the ligand. We emphasize that ultrasensitivity can also arise if K_a increases only as a convex function of n, for instance, as a power of n. Although cooperativity from this type of dependence necessarily has a lower Hill coefficient, the overall approach can nevertheless be expanded to include a wider class of interactions, such as those in which motion of the individual ligand site is more restricted.

Parameters Derived from Experiments

We now apply the general model derived above (Equation 9) to the Sic1-Cdc4 interaction, which shows a sharp inflection between five and six phosphorylation sites. A reasonable estimate for the average value of the dissociation constant $K_d = k_{-1}/k_1$ for each individual CPD site in Sic1 is 100 μM [17]. From Equations 3a and 3b, we get $k_{on}(1)/k_{off} = 9.246 \times 10^{-3} \times k_1/k_{-1} = 9.246 \times 10^{-3}$ mol $L^{-1} \times 10^4$ mol^{-1} L = 92.46. Note that this number, in contrast to K_d, represents an equilibrium of a first-order reaction, B ↔ P, and thus is dimensionless. This value suggests that the rate for P → B is two orders of magnitudes larger than that for B → P in the case of one ligand site (i.e., an individual CPD site) and three orders of magnitude in the case of seven ligand sites. Thus, Sic1 appears to spend on average at least 2–3 orders of magnitude longer time periods in state B than in state P, and whether one uses [B] or [B] + [P] in Equation 10 as the concentration of bound ligand, the result should be similar. A calculation of $k_{cap} = 4\pi r(D + D_R)N_A$ gives the estimate 2.65×10^6 m^3 mol^{-1} s^{-1} or 2.65×10^9 mol^{-1} L s^{-1} (D and D_R are both 5×10^{-11} m^2 s^{-1}, r = 35 Å). To determine a reasonable value for the rate constants $k_{esc}(1)$, we require that for n = 1 the model summarized in Equation 9 coincides with the standard model for equilibrium binding. We thus require that $(1 + 1 \times k_{on}(1)/k_{off})k_{cap}/k_{esc}(1) = 1/K_d(1)$ or $k_{esc}(1) = (1 + k_{on}(1)/k_{off})k_{cap} \times K_d(1) = (1 + 92.46) \times 2.65 \times 10^9 \times 10^{-4} = 2.48 \times 10^7$ s^{-1}. Here, we make the assumption that Sic1 with one ligand site has the same equilibrium constant as a peptide fragment.

We now compare this value for $k_{esc}(1)$ to expression (Equation B.19). Using Equations 3b, B.19, a range for k_1 of 10^7–10^{11} mol^{-1} L s^{-1}, r = 35 Å, and $D = 5 \times 10^{-11}$, we can derive values for k_{esc} (Figure 4B). Importantly, for the question of ultrasensitivity, when k_1 lies between 10^8 and 10^{10}, the model expression for $k_{esc}(n)$ is highly sensitive to n. It is also noteworthy that $k_{esc}(n)$ is only sensitive to the value of k_1 inside this range; it is equal to the unconstrained diffusion rate when k_1 is less than 10^8 and equal to 0 for a k_1 greater than 10^{10}. There is good agreement between the asymptotic value of $k_{esc}(1)$ calculated by using Equation B.19 with the previously derived value.

In the absence of experimentally determined values, the critical question of how the transition for Sic1 binding to Cdc4 is set at between five and six sites cannot be definitely answered. However, it is possible to make further assumptions in order to model this curve. Assuming a reasonable on rate for one site, $k_{on}(1) = 5.54 \times 10^7$, corresponding to $k_1 = 6 \times 10^9$ and a concentration of receptor in excess, [Cdc4] = [R] = $[R_f]$ = 1 μM, Equation B.19 together with Equation 10 generates the curve shown in (Figure 5A), which indicates a switch-like property at 4–6 ligand sites. The position of the switch is quite sensitive to the concentration of free Cdc4 (i.e., $[R_f]$); in fact, it is obvious from Equation 10 that 50% binding occurs when $K_a(n) = 1/[R_f]$.

Sensitivity to Choice of Parameters

The parameters r and k_{on} play a prominent role, but are difficult to assign precise values to, either through theoretical analysis or experimental data. It is therefore important to ask to what extent our analysis is sensitive to the specific estimates of these parameters. An increase in the value of r decreases the local concentration of binding sites but also increases the length of time a ligand stays inside the sphere. As these two effects tend to counteract each other, the outcome is not heavily influenced by the choice of r, as can be seen through comparison of Figures 5A–5C. In contrast, the analysis is very sensitive to the choice of $k_{on}(1)$, assuming a constant ratio $k_{on}(1)/k_{off}$ and D. For instance, a decrease of $k_{on}(1)$ by only a factor of three effectively eliminates the ultrasensitive response (Figure 5D). However, it is readily deduced from Equations 4, B.19, and 9 that it is the ratio $k_{on}(1)/D$ that matters. A critical test of the model therefore depends on the experimental determination of k_{on} and D.

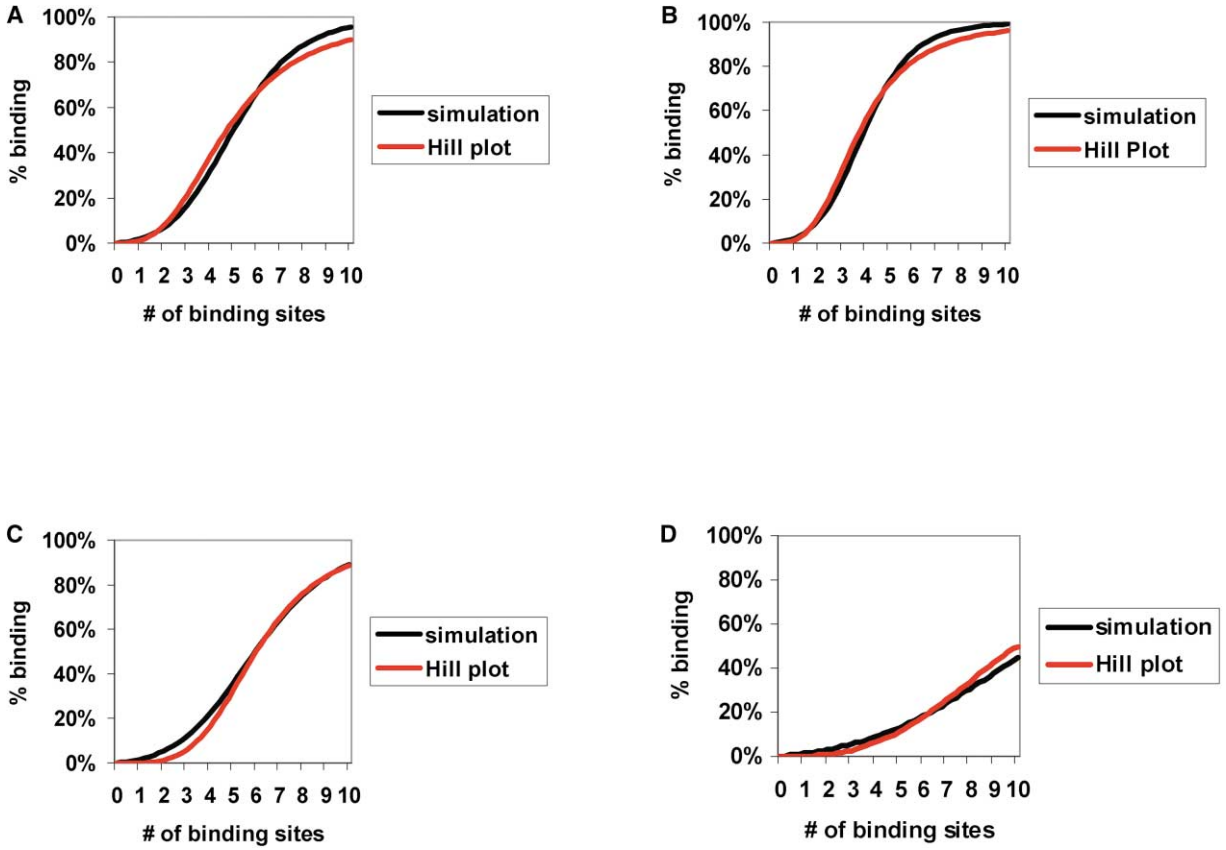

Figure 5. Cooperative Binding Curves for Allovalent Interactions over a Range of Parameter Values

(A) Cdc4 present in excess (1 μM) with r = 35 Å, $\omega = 4.08 \times 10^{-8}$ s, $k_{on}(1)/k_{off} = 92.46$, $k_{cap} = 2.65 \times 10^{9}\ M^{-1}\ s^{-1}$, $k_1 = 6 \times 10^{9}\ M^{-1}\ s^{-1}$, $k_{on}(1) = 5.54 \times 10^{7}\ s^{-1}$. A Hill plot with a coefficient of 2.9 and $S_{50} = 4.7$ is shown for comparison.

(B) Cdc4 present in excess (1 μM) with r = 25Å, $\omega = 2.08 \times 10^{-8}$ s, $k_{on}(1)/k_{off} = 253.7$, $k_{cap} = 1.89 \times 10^{9}\ M^{-1}\ s^{-1}$, $k_1 = 6 \times 10^{9}\ M^{-1}\ s^{-1}$, $k_{on}(1) = 1.52 \times 10^{8}\ s^{-1}$. A Hill plot with a coefficient of 3.2 and $S_{50} = 3.7$ is shown for comparison.

(C) Cdc4 present in excess (1 μM) with r = 45Å, $\omega = 6.75 \times 10^{-8}$ s, $k_{on}(1)/k_{off} = 43.50$, $k_{cap} = 3.41 \times 10^{9}\ M^{-1}\ s^{-1}$, $k_1 = 6 \times 10^{9}\ M^{-1}\ s^{-1}$, $k_{on}(1) = 2.62 \times 10^{7}\ s^{-1}$. A Hill plot with a coefficient of 4.0 and $S_{50} = 6.0$ is shown for comparison.

(D) Cdc4 present in excess (1 μM) with r = 35Å, $\omega = 4.08 \times 10^{-8}$ s, $k_{on}(1)/k_{off} = 92.46$, $k_{cap} = 2.65 \times 10^{9}\ M^{-1}\ s^{-1}$, $k_1 = 2.0 \times 10^{9}\ M^{-1}\ s^{-1}$, $k_{on}(1) = 1.85 \times 10^{7}\ s^{-1}$. A Hill plot with a coefficient 3.0 and $S_{50} = 10.0$ is shown for comparison.

Discussion

We have developed a general mathematical model that describes the interaction between a polyvalent disordered ligand and a single receptor site. We refer to this type of interaction as allovalent to reflect the fact that a binding site may be contributed from any one of numerous locations within the ligand at any given moment. The allovalent model provides a basis for understanding the complex phosphorylation-dependent interaction between the CDK inhibitor Sic1 and its cognate targeting subunit Cdc4 [17]. Perhaps counter to intuition, allovalent interactions are predicted to show a cooperative dependence on the number of interaction sites in the ligand, without the need to invoke thermodynamic concepts such as incremental increases in enthalpy or entropy that might in principle occur as more ligand sites are added. Substitution of reasonable values for the critical parameters in the Sic1-Cdc4 interaction yields a cooperative binding curve (Figure 5A) that fits well with existing qualitative binding data for Sic1 [17]. To critically test the model, it will be necessary to assign definitive values for r, k_1, and k_{-1} in the Sic1-Cdc4 interaction.

An important assumption in the above analysis is that binding sites on the polyvalent ligand move independently of each other and thus have ready access to the receptor binding site in the proximate state. This feature is probably close to the actual situation for completely unstructured molecules such as Sic1. If the hydrodynamic radius of Sic1 is approximately 30 Å and the hydrodynamic radius of a single binding site is one-tenth of that, or 3 Å, then according to the Stoke-Einstein equation, the diffusion coefficient of the fragment would be one-tenth of that of the full protein. This would translate into a relative mean traversed distance difference of $10^{1/2}$, or about 3-fold, for an individual site compared to that of a protein. Thus, an individual site can in principle diffuse from the center to the periphery, back to the center, and then back out to the periphery while the full protein diffuses out of the sphere.

The question of whether the model can be extended to systems with more constraints is hard to answer at this point. For example, in a globular protein with multi-

ple binding sites on its surface, the additional rotation for diffusion-limited access might substantially decrease k_{on} and thereby limit or even eliminate potential cooperative effects. In addition, the rebinding probability might be expected to conform less with the exponential distribution. In particular, the unstructured nature of Sic1 may be critical for its cooperative interactions with Cdc4. On the other hand, as discussed, it is possible to have a switch-like response even if the escape rate, k_{esc}, declines slower than exponentially. This possibility may be open to experimental test through construction of conformationally constrained substrates for Cdc4. Another related question is what effect possible constraints on independent motion of the sites, as imposed by the polypeptide backbone, would have on the conclusion of the model. As such constraints would tend to restrict the volume that any neighboring site could occupy, the rebinding rate would increase to further reduce the escape rate and render dependence on n even more switch like. A final potentially critical assumption is that the ligand is recentered in the sphere upon entering the P state. It is likely that some degree of recentering arises from electrostatic interactions between Cdc4 and Sic1 [23], random walk constraints, and molecular crowding effects [26]. Although recentering is probably incomplete, the qualitative conclusions of our model do not depend critically on the first exit time value. That is, if the time to exit from P is of a certain uniform positive duration, then k_{esc} will increase exponentially.

In addition to the inherent propensity of a polyvalent ligand-single receptor interaction to generate a cooperative binding curve, other mechanisms may also contribute to the step-like transition of the Sic1-Cdc4 binding curve that occurs between five and six phosphorylation sites. An obvious possibility is that binding of Sic1 might involve simultaneous interaction with Cdc4 at two or more distinct sites. That is, Cdc4 might possess one or more secondary phosphopeptide binding sites in addition to the primary site. Although recent structural analysis of a Cdc4-CPD phosphopeptide complex indicates only a single CPD binding pocket [23], even extremely weak sites would contribute to binding affinity in a cooperative manner because an additive change in free energy of the interaction would result in an exponential change in the association constant. One difficulty with this possibility is that given an approximate K_d of 100 μM for a single phosphodegron [17], even a secondary site with a K_d on the order of only 1 mM would be predicted to yield an overall K_d of 0.1 μM if two ligand sites were engaged, since the overall K_d increases multiplicatively. In contrast, binding is not evident until six ligand sites are present [17]. To explain this effect in purely thermodynamic terms would require six interaction sites with an average K_d of 0.1 M, an interaction which in reality is so weak that it cannot be discerned from nonspecific interactions. For similar reasons, possible contributions from dimerization or multimerization of the Cdc4 complex seem unlikely to produce the observed high degree of cooperativity [17, 23]. It is also conceivable that nonspecific electrostatic interactions between the negatively charged phosphorylated residues on Sic1 and an extensive region of positive electrostatic potential around the CPD binding site might contribute to cooperative dependence on the extent of Sic1 phosphorylation [23]. However, this argument is undermined by the fact that elimination of basic residues adjacent to the CPD binding site on the surface of Cdc4 increases rather than decreases relative affinity [23]. Moreover, the role of electrostatic interactions in recruitment and/or activation of enzyme substrates, termed the "Circe effect," is contentious at best [30].

A second possible thermodynamic contribution might arise from the greater entropy of the cumulative bound states, as opposed to a single highly constrained bound state. The attendant lower entropic penalty for the collection of bound states would increase the free energy of the binding reaction. Although difficult to estimate precisely, it is a priori expected that the entropy of the system will increase only as the logarithm of the number of possible conformations, such that there is no exponential gain in binding affinity as the number of binding sites is increased. If W is the total number of conformations that a ligand can take with a specific site bound to the receptor, then when another site on the same ligand binds to the receptor, one would reasonably expect the number of conformations not to differ much from W. Thus, the total number of conformations would be approximately nW. In terms of partition functions (p.f.), if $Q = \Sigma \exp(-E_i/kT)$ is the p.f. for a peptide with one binding site, then the corresponding p.f. for n sites would be $Q_n = \Sigma n \times \exp(-E_i/kT) = nQ$. Since S varies as logW (and logQ), one would expect S to vary as log n, and therefore the entropic contribution to the Gibbs energy should also vary as log n. Based on these arguments, it seems unlikely that the observed cooperativity is dictated by minor additive enthalpic or entropic contributions. Precise thermodynamic measurements will be needed to validate such arguments.

Polyvalent interactions occur in many biological contexts, including antibody-antigen interactions, host-pathogen interactions, cell adhesion, and transcription complex assembly on DNA [1]. All of these interactions may be in part governed by allovalent effects to a greater or lesser extent. For example, polyvalent ligands are prevalent in cellular adhesion to the extracellular matrix, such that high local concentrations of weak binding sites might engender high-affinity interactions [31]. Indeed, the enhanced apparent binding affinity of leukocytes to substratum by convective flow has recently been modeled by using a first passage time approach [32]. It is also possible that analogous kinetic effects may facilitate cooperative interactions within one- and two-dimensional systems, such as between transcriptional regulators and multiple elements along promoter DNA sequences [33] or between monovalent lipid binding domains with their cognate lipid ligands in membrane compartments [34]. Although there have been many theoretical investigations of how ligands bind either one- or two-dimensional targets, in such models, the ligand reacts with multiple receptors over a large target area (see [35] and references therein). The analysis reported here differs substantially in both assumptions, i.e., the ligand bears unconstrained, uncorrelated multiple sites that access a single binding site, not multiple binding sites, and in terms of mathematical form, a first passage time analysis is used, as opposed to solution of differential equations that describe ligand encounter rates [35].

Finally, in the context of cell regulation, we note that many protein-protein interactions are controlled by modification on multiple sites, whether via phosphorylation, acetylation, methylation, ubiquitination, or other modifications [36, 37]. Yet often a single controlling modification site cannot be defined, nor are potential minor contributions from other sites properly assessed [38]. For example, although the interaction of mammalian cyclin E with its cognate F box protein hCdc4 has long been known to depend on a dominant phosphorylation site, T380, contributions from several other sites have recently been discovered [39, 40]. Analogous effects may also occur for phosphorylation-dependent degradation of the CDK inhibitor $p27^{Kip1}$ by the SCF^{Skp2} ubiquitin ligase [41] and for substrates of the $SCF^{\beta\text{-}TrCP/Slimb}$ ubiquitin ligase [42]; this suggests that cooperative effects in substrate recognition may be a theme in regulated proteolysis.

Conclusions

A previously undescribed mode of cooperativity, termed allovalency, is developed from kinetic principles and the concept of first exit time. Unlike conventional thermodynamic approaches, the model is able to account for the experimentally observed cooperative dependence on the number of phosphorylated sites of Sic1 in its interaction with a single phospho-epitope binding site on Cdc4. The first exit time approach may allow a description of allovalent interactions in numerous biological processes.

Supplemental Data

In the Supplemental Data, we derive an analytical expression for k_{esc} in terms of the Laplace transform of the first exit time, thereby enabling us to produce a formula that can be used for computation. Supplemental Data are available at http://www.current-biology.com/cgi/content/full/13/19/1669/DC1/.

Acknowledgments

We thank Jim Ferrell, Julie Forman-Kay, James Choy, Frank Sicheri, Michael Elowitz, Mark Ptashne, and Sharad Ramanathan for stimulating discussions and Ashton Breitkreutz for the model figure. This work was supported by grants from the National Cancer Institute of Canada, the Canadian Institutes of Health Research (CIHR), and the Protein Engineering Network Centres of Excellence to T.P. and M.T. T.P. is a Distinguished Scientist of the CIHR, and M.T. holds a Canada Research Chair in Biochemistry.

Received: May 30, 2003
Revised: August 7, 2003
Accepted: August 15, 2003
Published: September 30, 2003

References

1. Mammen, M., Choi, S.-K., and Whitesides, G.M. (1998). Polyvalent interactions in biological systems: implications for design and use of multivalent ligands and inhibitors. Angew. Chem. *37*, 2754–2794.
2. Goldbeter, A., and Koshland, D.E. (1984). Ultrasensitivity in biochemical systems controlled by covalent modification: interplay between zero-order and multistep effects. J. Biol. Chem. *259*, 14441–14447.
3. Goldbeter, A., and Koshland, D.E. (1981). An amplified sensitivity arising from covalent modification in biological systems. Proc. Natl. Acad. Sci. USA *78*, 6840–6844.
4. Ferrell, J.E. (1996). Tripping the switch fantastic: how a protein kinase cascade can convert graded inputs into switch-like outputs. Trends Biochem. Sci. *21*, 460–466.
5. Ferrell, J.E., and Machleder, E.M. (1998). The biochemical basis of an all-or-none cell fate switch in *Xenopus* oocytes. Science *280*, 895–898.
6. Tyson, J.J., Chen, K.C., and Novak, B. (2003). Sniffers, buzzers, toggles and blinkers: dynamics of regulatory and signaling pathways in the cell. Curr. Opin. Cell Biol. *15*, 221–223.
7. Ferrell, J.E. (2002). Self-perpetuating states in signal transduction: positive feedback, double-negative feedback and bistability. Curr. Opin. Cell Biol. *14*, 140–148.
8. Hammes, G.G. (2000). Thermodynamics and Kinetics for the Biological Sciences (New York: John Wiley & Sons).
9. Klotz, I.M. (1997). Ligand-Receptor Energetics (New York: John Wiley & Sons).
10. Koshland, D.E. (1996). The structural basis of negative cooperativity: receptors and enzymes. Curr. Opin. Struct. Biol. *6*, 757–761.
11. Mitchison, T.J. (1995). Evolution of a dynamic cytoskeleton. Philos. Trans. R. Soc. Lond. B Biol. Sci. *349*, 299–304.
12. Yaffe, M.B., and Elia, A.E. (2001). Phosphoserine/threonine-binding domains. Curr. Opin. Cell Biol. *13*, 131–138.
13. Eck, M.J., Pluskey, S., Trub, T., Harrison, S.C., and Shoelson, S.E. (1996). Spatial constraints on the recognition of phosphoproteins by the tandem SH2 domains of the phosphatase SH-PTP2. Nature *379*, 277–280.
14. Dunker, A.K., Lawson, J.D., Brown, C.J., Williams, R.M., Romero, P., Oh, J.S., Oldfield, C.J., Campen, A.M., Ratliff, C.M., Hipps, K.W., et al. (2001). Intrinsically disordered protein. J. Mol. Graph. Model. *19*, 26–59.
15. Dyson, H.J., and Wright, P.E. (2002). Coupling of folding and binding for unstructured proteins. Curr. Opin. Struct. Biol. *12*, 54–60.
16. Wright, P.E., and Dyson, H.J. (1999). Intrinsically unstructured proteins: re-assessing the protein structure-function paradigm. J. Mol. Biol. *293*, 321–331.
17. Nash, P., Tang, X., Orlicky, S., Chen, Q., Gertler, F.B., Mendenhall, M.D., Sicheri, F., Pawson, T., and Tyers, M. (2001). Multisite phosphorylation of a CDK inhibitor sets a threshold for the onset of DNA replication. Nature *414*, 514–521.
18. Verma, R., Annan, R.S., Huddleston, M.J., Carr, S.A., Reynard, G., and Deshaies, R.J. (1997). Phosphorylation of Sic1p by G1 Cdk required for its degradation and entry into S phase. Science *278*, 455–460.
19. Skowyra, D., Craig, K.L., Tyers, M., Elledge, S.J., and Harper, J.W. (1997). F-box proteins are receptors that recruit phosphorylated substrates to the SCF ubiquitin-ligase complex. Cell *91*, 209–219.
20. Feldman, R.M., Correll, C.C., Kaplan, K.B., and Deshaies, R.J. (1997). A complex of Cdc4p, Skp1p, and Cdc53p/cullin catalyzes ubiquitination of the phosphorylated CDK inhibitor Sic1p. Cell *91*, 221–230.
21. Schwob, E., Bohm, T., Mendenhall, M.D., and Nasmyth, K. (1994). The B-type cyclin kinase inhibitor $p40^{SIC1}$ controls the G1 to S transition in *S. cerevisiae*. Cell *79*, 233–244.
22. Pawson, T. (1995). Protein modules and signalling networks. Nature *373*, 573–580.
23. Orlicky, S., Tang, X., Willems, A., Tyers, M., and Sicheri, F. (2003). Structural basis for phosphodependent substrate selection and orientation by the SCF^{Cdc4} ubiquitin ligase. Cell *112*, 243–256.
24. Tinoco, I., Sauer, K., and Wang, J.C. (1995). Physical Chemistry: Principle and Applications in Biological Sciences (New York: Prentice Hall).
25. Penkett, C.J., Redfield, C., Jones, J.A., Dodd, I., Hubbard, J., Smith, R.A., Smith, L.J., and Dobson, C.M. (1998). Structural and dynamical characterization of a biologically active unfolded fibronectin-binding protein from *Staphylococcus aureus*. Biochemistry *37*, 17054–17067.
26. Ellis, R.J. (2001). Macromolecular crowding: obvious but underappreciated. Trends Biochem. Sci. *26*, 597–604.
27. Atkins, P. (1998). Physical Chemistry (New York: W.H. Freeman).
28. Redner, S. (2001). A Guide to First-Passage Processes (Cambridge: Cambridge University Press).
29. Torquato, S., Kim, I.C., and Cule, D. (1999). Effective conductiv-

ity, dielectric constant, and diffusion coefficient of digitized composite media via first-passage equations. J. App. Physics *85*, 1560–1571.

30. Warshel, A., Florian, J., Strajbl, M., and Villa, J. (2001). Circe effect versus enzyme preorganization: what can be learned from the structure of the most proficient enzyme? Chembiochem *2*, 109–111.
31. Kiessling, L.L., Gestwicki, J.E., and Strong, L.E. (2000). Synthetic multivalent ligands in the exploration of cell-surface interactions. Curr. Opin. Chem. Biol. *4*, 696–703.
32. Chang, K.C., and Hammer, D.A. (1999). The forward rate of binding of surface-tethered reactants: effect of relative motion between two surfaces. Biophys. J. *76*, 1280–1292.
33. Berg, O.G., Winter, R.B., and von Hippel, P.H. (1981). Diffusion-driven mechanisms of protein translocation on nucleic acids. 1. Models and theory. Biochemistry *20*, 6929–6948.
34. Yaffe, M.B. (2002). The p47phox PX domain. Two heads are better than one! Structure *10*, 1288–1290.
35. Lagerholm, B.C., and Thompson, N.L. (1998). Theory for ligand rebinding at cell membrane surfaces. Biophys. J. *74*, 1215–1228.
36. Pawson, T., and Nash, P. (2000). Protein-protein interactions define specificity in signal transduction. Genes Dev. *14*, 1027–1047.
37. Jenuwein, T., and Allis, C.D. (2001). Translating the histone code. Science *293*, 1074–1080.
38. Cohen, P. (2000). The regulation of protein function by multisite phosphorylation: a 25 year update. Trends Biochem. Sci. *25*, 596–601.
39. Strohmaier, H., Spruck, C.H., Kaiser, P., Won, K.A., Sangfelt, O., and Reed, S.I. (2001). Human F-box protein hCdc4 targets cyclin E for proteolysis and is mutated in a breast cancer cell line. Nature *413*, 316–322.
40. Welcker, M., Singer, J., Loeb, K.R., Grim, J., Bloecher, A., Gurien-West, M., Clurman, B.E., and Roberts, J.M. (2003). Multisite phosphorylation by Cdk2 and GSK3 controls cyclin E degradation. Mol. Cell *12*, 381–392.
41. Malek, N.P., Sundberg, H., McGrew, S., Nakayama, K., Kyriakides, T.R., Roberts, J.M., and Kyriakidis, T.R. (2001). A mouse knock-in model exposes sequential proteolytic pathways that regulate $p27^{Kip1}$ in G1 and S phase. Nature *413*, 323–327.
42. Lefers, M.A., and Holmgren, R. (2002). Ci proteolysis: regulation by a constellation of phosphorylation sites. Curr. Biol. *12*, R422–R423.